Motor pool position and target topography regulated by β- and γ-catenin activities

Elena Y. Demireva[1], **Lawrence S. Shapiro**[2], **Thomas M. Jessell**[1,2], and **Niccolò Zampieri**[1]

[1]Howard Hughes Medical Institute, Kavli Institute for Brain Science, Dept. of Neuroscience, Columbia University, New York, NY 10032

[2]Dept. of Biochemistry and Molecular Biophysics, Columbia University, New York, NY 10032

Summary

Neurons typically settle at positions that match the location of their synaptic targets, creating topographic maps. In the spinal cord the organization of motor neurons into discrete clusters is linked spatially to the location of their muscle targets, establishing a topographic map of punctate design. To define the significance of motor pool organization for neuromuscular map formation we assessed the role of cadherin-catenin signaling in motor neuron positioning and limb muscle innervation. We find that joint inactivation of β- and γ-catenin scrambles motor neuron settling position in the spinal cord but fails to erode the predictive link between motor neuron transcriptional identity and muscle target. Inactivation of N-cadherin perturbs pool positioning in similar ways, albeit with reduced penetrance. These findings reveal that cadherin-catenin signaling directs motor pool patterning and imposes topographic order on an underlying identity-based neural map.

Introduction

In many regions of the central nervous system (CNS) the assembly of neurons into functional networks adheres to a preordained plan in which the identity and/or location of an individual neuron is inexorably linked to the position of its synaptic target - creating a neural map. Highly ordered maps, typified by retinal projections in the visual system, exhibit a continuously graded topography that links the position of neuronal cell bodies and synaptic targets along linear axes (Sperry, 1963; Luo and Flanagan, 2007). A second class of topographic maps, exemplified by the divergent projections of nuclear subgroups in the amygdala (Pitkanen et al., 1997), assigns neuronal cell body position in punctate rather than linear coordinates, yet preserves the predictive link between neuronal position and innervation target. For a third class of maps, notably those found in olfactory systems, topography is cast aside and molecular identity rather than position binds sensory neurons to their target structures (Imai et al., 2010). For topographic maps, however, it remains unclear if the precise positioning of neurons is a critical element in the formation of target connections, or is merely an incidental byproduct of circuit assembly.

Correspondence: tmj1@columbia.edu.

The spatial order of CNS neurons is readily apparent in the spinal cord, where motor neurons serving different biomechanical functions are organized into circumscribed groups, each occupying an invariant location. The precision of motor neuron positioning is at its most intricate for circuits that control limb movement: each of the fifty or so muscles used in locomotion and object manipulation receives input from a dedicated set of motor neurons whose cell bodies are clustered into stereotypic pools (Romanes, 1964; Vanderhorst and Holstege, 1997). The constancy of motor pool positioning has potential implications for the assembly of sensory-motor circuits - motor neuron position is predictive of sensory input specificity (Ladle et al., 2007), as well as the pattern of muscle target innervation (Landmesser, 1978). Thus, scrambling motor neuron position could uncouple the link between identity and muscle target or simply downgrade neuromuscular mapping to a state in which identity but not position is aligned with target connectivity. To date, however, it has not been possible to manipulate the position of motor neurons in a manner subtle enough to permit analysis of consequent alterations in patterns of target innervation.

We reasoned that defining cell surface recognition complexes that control the segregation and settling of spinal motor neurons, and then disrupting them genetically, could provide one way of assessing the influence of neuronal position on motor circuit organization. Classical cadherins represent a prominent family of adhesion proteins expressed by spinal motor neurons (Price and Briscoe, 2004). Manipulation of type II cadherin expression profiles in chick embryos disrupts the normal settling pattern of motor pools (Price et al., 2002; Patel et al., 2006). Nevertheless, mice in which individual type II cadherins have been eliminated genetically exhibit no obvious defects in motor neuron positioning (E.Y.D., S.Price, N.Z., and T.M.J. unpublished observations). Given the diversity of type II cadherins expressed by motor neurons (Price et al., 2002; this study), it is possible that residual profiles of cadherin expression are sufficient to maintain molecular and spatial distinctions between motor neuron subsets. Moreover, type I cadherins expressed by spinal motor neurons (Zelano et al., 2006) could also participate in motor neuron sorting.

To circumvent the cadherin diversity problem we turned our attention to catenins, the primary intracellular transducers of classical cadherin-mediated adhesion and recognition (Kemler, 1993; Nelson, 2008). Within the catenin family, the activities of β- and γ-catenin can be distinguished from those of α- and δ-catenin on the basis of different modes of interaction with the cytoplasmic domain of cadherins (Huber and Weis, 2001). β-catenin is the most widely studied mediator of classical cadherin signaling, although γ-catenin has similar activities in certain non-neural cell types (Butz et al., 1992; Zhurinsky et al., 2000). But there has been no systematic exploration of the respective roles of β- and γ-catenin as mediators of cadherin signaling in the developing CNS, nor of their potential role in motor neuron positioning and target connectivity.

In this study we sought to inactivate the cadherin-catenin signaling pathway in spinal motor neurons as a way of assessing the significance of motor neuron position in aspects of motor circuit assembly. Our analysis of mice in which key components of cadherin-catenin signaling have been perturbed genetically reveals that inactivation of β- and γ-catenin jointly but not individually, and to a lesser extent of N-cadherin, disrupts motor neuron positioning. This degradation of positional order fails to undermine the predictive link between transcriptional identity, axonal trajectory and muscle target selectivity. Thus the clustering and positioning of cell bodies is not required for motor neuron subtypes to innervate appropriate target muscles. Nevertheless, the emergence of neuromuscular maps of topographic rather than identity-based design is dependent on cadherin-catenin signaling.

Results

Overlapping expression of β- and γ-catenin in spinal motor neurons

To assess the involvement of catenins in motor neuron positioning and target topography we examined β- and γ-catenin expression profiles in mouse spinal cord between embryonic day (e) 9.5 and post-natal day (p) 0.

Broad expression of β-catenin mRNA and protein was detected from e9.5 (Figure 1A and 1B; Figure S1A and S1B). In embryonic motor neurons marked by GFP expression in *Hb9::*GFP transgenic mice (Wichterle et al., 2002), β-catenin protein was expressed at high levels on the cell surface, but at negligible levels in the cytoplasm (Figure 1E and 1F). From e10.5 to e11.5, expression of γ-catenin was restricted to motor neurons, although blood vessels were labeled (Figure 1C, 1D, 1M and 1N). From e12.5 onwards, γ-catenin was also expressed by neurons in other domains of the spinal cord (Figure S1C and S1D). In motor neurons γ-catenin protein was detected at highest levels in association with the cell surface, with lower levels in the cytoplasm (Figure 1G and 1H). Thus, β- and γ-catenin are co-expressed by spinal motor neurons as they settle in distinct positions and establish axonal trajectories.

Eliminating β- and γ-catenin from spinal motor neurons

We evaluated the impact of inactivating β- and γ-catenin genes from motor neurons. In mouse embryos, β-catenin activity is required at early developmental stages and constitutive *β-catenin* mutants die before motor neuron generation (Haegel et al., 1995). To bypass this early requirement we crossed mice carrying two copies of a floxed *β-catenin* (β-cat$^{flox/flox}$) allele (Brault et al., 2001) with an *Olig2::Cre* driver line that directs recombination in motor neuron progenitors (Dessaud et al., 2007), to generate $\beta^{\Delta MN}$ mice. We found that over 90% of motor neurons in $\beta^{\Delta MN}$ mice lacked β-catenin transcript at e13.5, with no obvious loss from other spinal cells (Figure 1I–L), and mutant mice died within 24h of birth (Table S1). Constitutive *γ-catenin* ($\gamma^{-/-}$) mutant mice (Ruiz et al., 1996) died between e10.5 and e15.5 from heart defects (Table S1), and revealed a complete loss of γ-catenin mRNA and protein from embryonic motor neurons and other spinal cord cells (Figure 1M–P).

We generated *β-* and *γ-catenin* double mutant ($\beta^{\Delta MN}\gamma^{-/-}$) embryos by introducing constitutive *γ-catenin* mutant alleles into an *Olig2::Cre$^{+/-}$*; *β-cat$^{flox/flox}$* background. Recombined $\beta^{\Delta MN}\gamma^{-/-}$ embryos were detected at lower than predicted (1:16) Mendelian frequencies: ~1:30 at e10.5 and ~1:44 at e13.5. We attempted to extend the viability of catenin double mutant embryos through the generation and use of a conditional *γ-catenin* mutant allele (*γ-cat^{flox}*; Figure S1M–O). Crossing *Olig2::Cre* and *γ-cat$^{flox/flox}$* mice produced embryos in which γ-catenin protein was eliminated preferentially from motor neurons (Figure S1P–S). But recombined *Olig2::Cre$^{+/-}$*; *γ-cat$^{-/flox}$; β-cat$^{flox/flox}$* ($\beta^{\Delta MN}\gamma^{\Delta MN}$) double conditional mutants survived only until e14.5 (Table S1), limiting analysis of motor neuron differentiation to defects evident by this developmental stage.

Motor neuron columnar segregation in β- and γ-catenin mutant embryos

We first assessed the impact of catenin activity on motor neuron differentiation through analysis of phenotypes in *β-* and *γ-catenin* single, and $\beta^{\Delta MN}\gamma^{-/-}$ double mutant embryos. Motor neuron columnar classes (Figure 2A) were identified by transcription factor expression profiles (Dasen et al., 2008). At lumbar levels, lateral motor column (LMC) neurons express FoxP1 whereas median motor column (MMC) neurons express Lhx3. At thoracic levels, hypaxial motor column (HMC) neurons co-express Hb9 and Isl1/2 but not FoxP1 or Lhx3, and preganglionic column (PGC) neurons co-express nNOS and pSMAD.

The total number of spinal motor neurons generated from e10.5 to e13.5 was similar in control, β- and γ-catenin single mutant, and $\beta^{\Delta MN}\gamma^{-/-}$ double mutant embryos (Table S2). Although the number of LMC, HMC and PGC neurons was similar in $\beta^{\Delta MN}\gamma^{-/-}$ and control embryos, we detected a ~25% reduction in the number of MMC neurons in $\beta^{\Delta MN}\gamma^{-/-}$, as well as in single β-catenin mutants (Figure 2F and Table S2). In addition, we observed that in $\beta^{\Delta MN}\gamma^{-/-}$ embryos ~15% of motor neurons, primarily MMC neurons, failed to migrate away from the ventricular zone (Figure 2C, S2A and Table S3). Nevertheless, the number of post-migratory LMC, HMC and PGC neurons was similar in $\beta^{\Delta MN}\gamma^{-/-}$ and control embryos (Figure 2F). Moreover, LMC and HMC neurons remained segregated from MMC neurons at lumbar and thoracic levels, respectively (Figure 2B–E; data not shown). In contrast, PGC neurons were scattered in ectopic ventral positions in e13.5 $\beta^{\Delta MN}\gamma^{-/-}$ embryos (Figure 2H–I, and S2B). Thus, despite the disruption in MMC and PGC organization, the specification, lateral migration, and segregation of LMC neurons are little affected by the loss of β- and γ-catenin activities.

Although LMC neurons remain segregated from other columnar subtypes, we observed that the area of the ventral spinal cord occupied by the LMC was ~20% greater in $\beta^{\Delta MN}\gamma^{-/-}$ than in control embryos, and the packing density of FoxP1+ LMC neurons was reduced (Figure 2J–K and 2G). However overall neuronal packing density within the confines of the LMC, defined by NeuN expression was unchanged (Figure 2J–K and 2G), implying that other neuronal classes have encroached the boundaries of the LMC. Consistent with this, we detected a ~2.5 fold increase in the number of En1+ V1 interneurons and a ~3 fold increase in Chx10+ V2a interneurons within the confines of the LMC in $\beta^{\Delta MN}\gamma^{-/-}$ embryos (Figure S2C–L). Thus, the erosion of LMC cohesion elicited by loss of β- and γ-catenin activities permits intercalation of ventral interneurons.

β- and γ-catenin activities required for LMC divisional segregation and pool sorting

We examined whether the segregation of LMC neurons is affected by the loss of β- and γ-catenin activities. In $\beta^{\Delta MN}\gamma^{-/-}$ embryos we observed a marked intermixing of medial and lateral LMC neurons, evident by e11.5 (Figure 3A and 3B). We devised a divisional mixing index (D_{mi}) to monitor the extent to which Isl1+ medial (M) LMC neurons invade the confines of the HB9+ lateral (L) LMC division, and vice versa. In control e13.5 embryos we observed a relatively low incidence of inter-divisional mixing (D_{mi}: M→L 0.23, L→M 0.30; Figure 3C, 3E, 3G and 3H). In $\beta^{\Delta MN}\gamma^{-/-}$ embryos we detected a ~2.5 to 3 fold increase in D_{mi} values (D_{mi}: M→L 0.70, L→M 0.71; p<0.0001, vs control embryos; Figure 3D, 3F, 3G and 3H). D_{mi} values in β- and γ-catenin single mutants were similar to those in control embryos (data not shown). Thus, β- and γ-catenin activities promote the divisional segregation of LMC neurons.

We next examined whether β- and γ-catenin are required for the clustering and segregation of motor pools. We focused on motor pool complexes that occupy medial or lateral LMC divisions and are identifiable by expression of homeodomain and ETS transcription factors (De Marco Garcia and Jessell, 2008). The adductor/gracilis (A/G) pool complex was identified by co-expression of Nkx6.1 and Er81; hamstring (H) pools by expression of Nkx6.1; vasti (V) pools by expression of Er81, and the rectus femoris/tensor fasciae latae (R/T) pool complex by expression of Nkx6.2 (Figure 3I and 3K). We detected no change in the number of motor neurons allocated to these pool complexes in $\beta^{\Delta MN}\gamma^{-/-}$ embryos (data not shown).

To provide a quantitative assessment of motor pool organization we used a pool mixing index $\beta^{\Delta MN}\gamma^{-/-}$ embryos. We first assessed the (P_{mi}) to document neuronal neighbor identities in control and impact of β- and γ-catenin inactivation on the clustering of motor pools that reside in different LMC divisions, analyzing the segregation of lateral R/T from

medial H pools. In control embryos R/T neurons were clustered in a position lateral to H neurons and exhibited a low incidence of intermixing ($P_{mi [H \to R/T]}$ 0.32; Figure 3I, 3K, and 3M). In $\beta^{\Delta MN}\gamma^{-/-}$ embryos, R/T neurons were no longer clustered or laterally restricted, and were intermingled with H neurons, with P_{mi} values ~3-fold greater than control ($P_{mi [H \to R/T]}$ 0.88, p <0.0001 vs control; Figure 3J, 3L, and 3M). A similar analysis of intermixing between R/T and values in $\beta^{\Delta MN}\gamma^{-/-}$ embryos (Table S4). We did not A/G pool complexes revealed a ~3 fold increase in P_{mi} observe inter-divisional mixing of R/T and H pools in single β- and γ-catenin mutants (Table S4). Thus, neurons in motor pools that normally occupy different LMC divisions are intermingled in catenin mutants, a result consistent with divisional intermixing.

We also examined whether the clustering and positioning of motor pools that reside within a single (lateral) LMC division are affected by the loss of β- and γ-catenin activities. In control embryos neurons in R/T and V pools were tightly clustered and exhibited little intermixing ($P_{mi [V \to R/T]}$ 0.26; Figure 3K and 3M) whereas in $\beta^{\Delta MN}\gamma^{-/-}$ embryos neurons in these two pools were more scattered and extensively intermingled ($P_{mi [V \to R/T]}$ 0.66; p <0.0001 vs control; Figure 3L, and 3M). Intra-divisional mixing of these pools was not observed in β- and γ-catenin single mutants (Table S4). Thus, the segregation of motor pools that normally occupy the same LMC division is also disrupted by the loss of motor neuron β- and γ-catenin activities. In addition, we examined whether there are defects in motor pool position along the rostro-caudal axis of the spinal cord. Analysis of the position of molecularly defined motor pools at lumbar levels 2 (L2), L3 and L4 revealed that their rostro-caudal limits were preserved in $\beta^{\Delta MN}\gamma^{-/-}$ embryos (Figure S3). Thus, β- and γ-catenin activities control intra-segmental but not rostro-caudal pool organization.

Motor pool identity still predicts muscle target in β- and γ-catenin mutants

We next asked whether the disruption in motor pool positioning that accompanies the loss of β- and γ-catenin activities erodes the predictive link between motor neuron transcriptional identity, axonal trajectory and limb muscle innervation.

The overall pattern and fasciculation of GFP$^+$ motor nerves was similar in the hindlimbs of control and $\beta^{\Delta MN}\gamma^{-/-}$ embryos that carried an *Hb9::*GFP allele (Figure S4A–B). This finding permitted us to probe the link between LMC divisional identity and axonal trajectory. We therefore monitored the transcriptional status of motor neurons retrogradely-labeled after focal rhodamine-dextran (Rh-D) tracer injection into the dorsal or ventral halves of the hindlimb. After ventral Rh-D injection in control or $\beta^{\Delta MN}\gamma^{-/-}$ embryos, 98% and 97% respectively of labeled motor neurons expressed Isl1 - a medial LMC profile (Figure 4A–D). Conversely, after dorsal Rh-D injection in control and $\beta^{\Delta MN}\gamma^{-/-}$ embryos, 99% and 96% respectively of labeled motor neurons excluded Isl1 (Figure 4E–H). Thus, the loss of β- and γ-catenin activities does not perturb the link between the divisional identity of LMC neurons and the ability of axons to select appropriate dorso-ventral trajectories upon entering the limb.

We next examined whether the link between motor pool identity and muscle target selection is maintained under conditions of pool scrambling. In control and $\beta^{\Delta MN}\gamma^{-/-}$ embryos, 82% and 83% respectively, of LMC neurons labeled after Rh-D injection into the adductor magnus muscle appropriately co-expressed Isl1 and Nkx6.1 (Figure 4I–L), and 96% and 94% respectively, of LMC neurons labeled after Rh-D injection into the rectus femoris muscle appropriately co-expressed Hb9 and Nkx6.2 (Figure 4N–Q). We also addressed the possibility that in catenin mutants motor neurons might be able to project to correct muscle targets only when they occupy positions coincident with normal pool location. As a consequence, we examined the spatial distribution of retrogradely-labeled motor neurons with reference to the total cohort of motor neurons within medial or lateral LMC divisions.

We found that retrogradely-labeled adductor magnus or rectus femoris motor neurons in $\beta^{\Delta MN}\gamma^{-/-}$ embryos were not confined to a localized subdomain, and many were positioned far from their normal pool epicenter (Figure 4M, R). Thus the ectopic positions of motor neuron in catenin mutants do not disturb the predictive link between molecular identity, axonal trajectory and target muscle specificity.

We also examined the impact of loss of β- and γ-catenin activities on early stages of motor neuron dendritic development, focusing on adductor motor neurons, which exhibit a stereotypic radial dendritic architecture. In control embryos the dendrites of adductor motor neurons, delineated by muscle Rh-D injection at e14.5, were elongated and possessed ~5 primary branch points (Figure S4C–D, and S4I–K). In $\beta^{\Delta MN}\gamma^{\Delta MN}$ embryos, both total dendritic length and primary branch number were reduced ~2–3 fold (Figure S4G–H, and S4I–K). Defects in dendritic length and branching were not observed in single *β*- and *γ-catenin* mutant backgrounds (Figure S4I–K). Thus β- and γ-catenin also act redundantly to control early stages of motor neuron dendritic growth.

Motor neuron catenin phenotypes do not involve Wnt signaling

Catenins have been implicated in Wnt as well as cadherin signaling (Nelson and Nusse, 2004). Defining which cell surface signaling pathways engage catenins requires an assessment of the respective contributions of Wnts and cadherins to motor neuron cell body positioning. The absence of motor pool positioning defects in single *β-catenin* mutants, a condition that abolishes Wnt signaling in many mammalian cell types (Grigoryan et al., 2008), already provides an argument against the involvement of Wnt signaling. Nevertheless, we used additional genetic strategies to examine whether embryonic motor neurons are exposed to Wnt signals, and whether their settling pattern is disrupted under conditions of deregulated Wnt signaling.

To assess whether embryonic motor neurons respond to Wnt activity we used a *BAT-gal* transgenic mouse line in which a β-catenin-sensitive LEF/TCF transcriptional response element directs β-galactosidase (β-gal) expression in cells exposed to Wnt signals (Maretto et al., 2003). Analysis of *BAT-gal* mice at e10.5 revealed that fewer than 5% of motor neurons expressed β-gal, and from e11.5 to e14.5 β-gal was not detected in any spinal motor neurons (Figure S5A–C′). In contrast, many dorsal cells expressed β-gal (Figure S5A–C′), consistent with the known role of Wnt signaling in promoting the proliferation of dorsal spinal progenitors (Megason and McMahon, 2002). We also studied mice in which the Wnt signaling pathway is constitutively activated by expression of a truncated β-catenin protein that accumulates in the nucleus and activates Wnt target genes, even in the absence of Wnt exposure (Harada et al., 1999). We used an *Olig2::Cre* driver to express the floxed *Catnb$^{lox(ex3)}$* constitutive allele selectively in motor neurons. Analysis of recombined *Catnb$^{lox(ex3)}$* mice at e13.5 revealed an expansion of the motor neuron progenitor domain (data not shown), probably a reflection of the initial phase of transgene expression and activity in motor neuron progenitors (Megason and McMahon, 2002). Nevertheless, we detected no change in the pattern of LMC columnar, divisional or pool segregation (Figure S5D–I). Together, these genetic manipulations argue against the idea that a disruption in Wnt signaling underlies the motor neuron phenotypes observed after loss of β- and γ-catenin activities.

Catenins regulate localization and function of classical cadherins

We next explored whether catenin regulation of LMC organization reflects the involvement of classical cadherins. The profile of expression of type I and type II cadherins is consistent with their involvement in motor neuron sorting. The type I cadherins *N-cadherin* (*N-cad*) and *R-cad*, the type II cadherins *cad-6*, *cad-7*, *cad-8*, *cad-9*, *cad-10*, *cad-11*, *cad-12*, *cad-20*

and *cad-22*, as well as the divergent classical cadherin *T-cad (cad-13)*, were expressed by spinal motor neurons between e10.5 and e15.5 (Figure S6). *N-cad, cad-6* and *cad-11* were expressed by all spinal motor neurons, with the remainder restricted to smaller subpopulations, such that individual motor columns and pools could be distinguished by cadherin expression profiles (Figure S6).

We examined whether the loss of β- and γ-catenin activities influences the localization of representative type I and II cadherins. In the spinal cord of e10.5 $\beta^{\Delta MN}\gamma^{-/-}$ mice we detected a marked reduction in the level of motor neuron surface N-cad (Figure 5A–D). We also detected a decrease in surface N-cad on cultured motor neurons isolated from $\beta^{\Delta MN}\gamma^{-/-}$ embryos, accompanied by a marked increase in intracellular accumulation of N-cad, primarily in the Golgi compartment (Figure 5K–L′ and 5Q). The subcellular localization of N-cad was not perturbed in *β-* or *γ-catenin* single mutants (data not shown). Cad-8 was expressed at high levels on the surface of control motor neurons (Figure 5M–M′, 5P and 5R) whereas in $\beta^{\Delta MN}\gamma^{-/-}$ embryos, cad-8 expression was detected primarily in the cytoplasm (Figure 5N–N′, 5P and 5R). Thus, catenins promote surface localization of classical cadherins in motor neurons.

We tested N-cad function by monitoring neurite outgrowth from motor neurons isolated from e10.5 *Hb9::GFP* control and $\beta^{\Delta MN}\gamma^{-/-}$ embryos, cultured on naïve or *N-cad* transfected CHO cells. Control motor neurons exhibited a ~2-fold increase in the length and branching of GFP$^+$ neurites when grown on *N-cad* transfected CHO cells, compared to control CHO cells (Figure 5E–F and 5I–J; p<0.01). In contrast, motor neurons derived from $\beta^{\Delta MN}\gamma^{-/-}$ embryos did not exhibit enhanced neurite outgrowth or branching on *N-cad* transfected CHO cells (Figure 5G–J). Thus, motor neurons require β- and γ-catenin activity for functional interaction with an N-cad cellular substrate. In contrast to N-cad substrates, we failed to detect an increase in neurite outgrowth when control motor neurons were grown on CHO cell lines stably expressing cad-6, cad-8 or cad-11 (data not shown), preventing us from evaluating the requirement for β- and γ-catenin in type II cadherin function.

N-cadherin inactivation results in catenin-like phenotypes

The role of catenins as mediators of N-cadherin activity *in vitro* led us to ask whether elimination of motor neuron N-cadherin generates LMC neuronal phenotypes that resemble those observed *in vivo* after catenin inactivation. We crossed an *Olig2::Cre* driver line with mice carrying two floxed *N-cadherin* (*N-cad$^{fl/fl}$*) alleles (Kostetskii et al., 2005), to generate *N-cad$^{\Delta MN}$* mice. Analysis of *N-cad$^{\Delta MN}$* embryos at e13.5 revealed a loss of N-cad expression from over 90% of motor neurons (Figure S7A–D).

Many aspects of LMC organization were unaffected. The initial lateral migration of LMC neurons, as well as their segregation from MMC neurons were resistant to the loss of motor neuron N-cadherin (Figure 6A). The expansion in LMC area observed in $\beta^{\Delta MN}\gamma^{-/-}$ embryos was not evident in *N-cad$^{\Delta MN}$* mutants, nor was there evidence of encroachment of V1 and V2a interneurons into the LMC domain (data not shown). Moreover the defects in motor neuron dendritic arborization observed upon β and γ-catenin inactivation were not evident in *N-cad$^{\Delta MN}$* mice (Figure S7I–K). But as with catenin mutants, we detected a defect in the migration and settling of PGC neurons in the intermediate spinal cord of *N-cad$^{\Delta MN}$* embryos (Figure S7F–H).

In addition, motor pool clustering and positioning was disrupted by inactivation of N-cadherin, albeit less severely than in catenin mutants (Figure 6A–D and 6K). In *N-cad$^{\Delta MN}$* embryos we detected a ~2-fold increase over controls in the incidence of mixing of medial and lateral LMC neurons (D_{mi}: L→M 0.45, L→M 0.55; p<0.0001, vs control embryos; Figure 6A–B). Analysis of inter-divisional pool mixing in *N-cad$^{\Delta MN}$* values embryos

revealed that R/T neurons were often intermingled with H neurons, with P_{mi} ~2-fold greater than those in control embryos ($P_{mi [H \to R/T]}$ 0.60, p<0.0001 vs control; Figure 6C–D and Table S4). In addition analysis of intra-divisional pool mixing in $N\text{-}cad^{\Delta MN}$ embryos showed that neurons in the R/T and V pools were intermingled ($P_{mi [V \to R/T]}$ 0.43; p<0.0001 vs control; Figure 6C–D and Table S4), although not to the extent observed in $\beta^{\Delta MN}\gamma^{-/-}$ embryos (Figure 6K). Despite the disorganization of motor pool positioning, retrograde labeling studies in $N\text{-}cad^{\Delta MN}$ embryos established that the link between motor neuron divisional and pool transcriptional identity and axonal trajectory was preserved (Figure 6E–J). These findings show that motor pool organization depends on N-cadherin function. They also indicate that, as with catenins, the mis-positioning of LMC neurons that accompanies inactivation of N-cadherin degrades neuromuscular mapping from a topographic to an identity-based plan.

Discussion

The settling position of spinal motor pools has been conserved for over three hundred million years of tetrapod evolution, an elaborate feat of neural cell patterning that ensures the topographic organization of circuits for limb movement. The molecular mechanisms that control motor pool settling and the fundamental rationale for positioning pools with such fidelity have remained obscure, however. We present genetic evidence that the clustering and positioning of motor pools in the spinal cord depends on the overlapping activities of β- and γ-catenin, and to an extent, on N-cadherin. We show that the loss of cadherin-catenin signaling erodes the predictive link between the position of a motor neuron cell body and the identity of its limb muscle target. But despite this breakdown in positional order, misplaced motor neurons continue to project to target muscles with a specificity that conforms to their transcriptional identity. Thus cadherin-catenin signaling provides a molecular foundation for the topographic design of spinal motor circuits.

Why expend developmental energy on motor neuron positioning if there is no beneficial impact on the precision of target muscle innervation? The clustering of motor neurons into pools presumably facilitates the formation of gap junction channels between neurons with a common muscle target, thereby enhancing the coherence of motor neuron firing that is thought to stabilize neuromuscular connections (Personius et al., 2007). In addition, recent studies indicate that motor pool positioning is a key step in the assignment of selective sensory-motor connectivity patterns (Surmeli et al., 2011). Proprioceptive sensory afferents from individual muscles project their axons to discrete tiers along the dorsoventral axis of the spinal cord independently of the subtype identity or presence of motor neurons (Surmeli et al., 2011). Thus an additional purpose of pool positioning may be to ensure that motor neurons receive functionally appropriate inputs from sensory, and perhaps also from central, neurons.

Cadherin-catenin signaling and the topographic design of neural maps

All neural maps conform to a basic organizational plan in which neuronal identity is matched with target position. The existence of neural maps that spurn the potential benefits of stereotypic cell body positioning (Luo and Flanagan, 2007; Imai et al., 2010) raises the issue of whether the positional invariance associated with topographic maps is instrumental in directing neurons of a particular molecular character to specific targets. Our genetic findings on the assembly of a spinal motor map show that the precise positioning of neuronal cell bodies is not a requisite step in map formation – the transcriptional identity of ectopic motor neurons still predicts muscle target. Rather elimination of cadherin-catenin signaling downgrades the topographic organization of this map to an identity-based scheme, similar to that which operates normally in olfactory sensory systems (Figure 7, Imai et al., 2010).

Our findings also address the rationale for constructing some neural maps with topographic, and others with identity-based, plans. Linear topographic mapping is associated with primary sensory systems in which systematically ordered features of the sensory world - visual receptive field space and auditory tonotopy - are represented in corresponding neural coordinates that facilitate downstream processing (Luo and Flanagan, 2007). In olfactory systems, where the rules of neuronal activation rely on selective chemical rather than spatially ordered stimuli (Imai et al., 2010), sensory maps adhere to an identity-based rather than topographic plan. Other topographic maps, such as the motor connections studied here, are constructed along punctuate rather than linear design principles. Punctate topographic maps appear restricted to neurons of central rather than peripheral origin, perhaps because CNS neurons receive synaptic inputs from diverse neuronal sources. Adherence to a punctate topographic design may therefore simplify the task of patterning neural inputs in a way that conforms to the functional organization of output pathways.

Embryological studies in chick have previously examined how the positional displacement of limb innervating motor neurons influences patterns of muscle connectivity. After limited rostrocaudal inversions of the spinal cord, motor axons enter the limb at inappropriate positions but still innervate correct muscle targets (Lance-Jones and Landmesser, 1980). In this experimental design the local environment of motor neuron cell bodies remained constant, thus testing the consequences of a peripheral axonal mismatch, rather than a change in motor neuron positional coordinates. Nevertheless, these studies, together with our genetic analysis, support the view that the molecular identity rather than position of an individual motor neuron determines its muscle target selectivity.

Cadherin-catenin signaling and the organization of motor pools

Our genetic findings show that the clustering and positioning of motor pools depend on the overlapping functions of β- and γ-catenin, whereas earlier stages of motor neuron migration and columnar segregation appear much less severely affected. Thus catenin signaling serves a critical and selective role in establishing the fine topographic organization of limb-innervating motor neurons. The redundant activities of β- and γ-catenin in motor neuron positioning is noteworthy, given that most studies on the role of catenins during CNS development have focused on β-catenin (Grigoryan et al., 2008). Our findings raise the possibility that γ-catenin also has a widespread role in neuronal patterning. The unappreciated involvement of γ-catenin could explain reported discrepancies in the impact of N-cadherin and β-catenin inactivation on programs of brain development. As one example, aspects of cortical neuronal differentiation appear more severely affected in N-cadherin than in β-catenin mutants (Machon et al., 2003; Kadowaky et al., 2007).

Our findings also imply that classical cadherins function as surface adhesion receptors that engage motor neuron catenins. The defects in motor pool clustering and positioning in N-cadherin mutants indicate a prominent role for this type I cadherin in the assembly of motor circuits. Nevertheless, the partial nature of pool mixing phenotypes observed after N-cadherin inactivation implies the involvement of additional catenin-dependent surface proteins (Figure 6K). Type II cadherins are the most likely candidates as additional membrane recruiters of motor neuron catenins. In chick spinal cord, motor pools can be distinguished by type II cadherin expression profiles, and gain and loss of function manipulations that normalize type II cadherin expression disrupt motor pool segregation (Price et al., 2002). The motor pool specificity of type II cadherin expression is also evident in mouse, indicating conservation in this molecular feature of motor neuron diversity. Nevertheless, the complexity of motor pool cadherin profiles has confounded genetic attempts to examine the logic of type II cadherin specificity. Thus we cannot exclude that other motor neuron surface proteins engage catenin signaling. Catenins have been shown to regulate the activity of nectins through indirect interactions via the actin cytoskeleton (Takai

et al., 2003). In addition, reelin signaling engages cadherins and regulates the settling position of PGC neurons (Yip et al., 2009; Jossin et al., 2011), and could have a secondary role in the positioning of limb-innervating motor neurons (Palmesino et al., 2010).

The role of N-cadherin in motor pool sorting, taken together with prior studies on type II cadherins (Price et al., 2002), argues that both main families of classical cadherins conspire in the control of motor neuron position. The nature of the joint involvement of type I and type II cadherins remains unclear, however. Higher order cadherin complexes are unlikely to contribute to motor neuron patterning, given structural data showing that type I/type II cadherin hetero-oligomers are prohibited (Patel et al., 2006). More likely, engagement of N-cadherin and perhaps broadly expressed type II cadherins such as cad-6 and cad-11 could provide a basal level of adhesion that primes neuronal responses to more selectively expressed type II cadherins.

Cadherin-catenin signaling reveals the compartmental nature of motor neuron patterning

Motor neurons can be distinguished from all other classes of neurons generated in the CNS by the fact that their axons extend into the periphery. As a consequence, motor circuit assembly demands that motor neurons establish functional connections with their target muscles in the context of peripheral cues, while their cell bodies and dendrites are patterned within a central matrix. The loss of catenin function perturbs the organization of motor pools, as well as dendritic arborization. In contrast, cadherin-catenin inactivation has no impact on the patterning of motor nerves in the limb, or on the selectivity of target muscle innervation. Thus there is a fundamental molecular distinction in the workings of the central and peripheral programs of motor circuit assembly.

The dedicated role of catenin signaling in the somato-dendritic patterning of motor neurons provides a counterpoint to recent studies on peripheral guidance cues for motor axons. Eph-mediated avoidance of ephrin ligands directs the dorso-ventral trajectory of LMC axons in the developing limb (Kania and Jessell, 2003; Luria et al., 2008). Yet the perturbation of Eph signaling has no impact on the divisional or pool segregation of LMC neurons (Kania and Jessell, 2003; Luria et al., 2008). Thus downstream of core transcriptional programs, topographic motor mapping appears to be mediated by compartmentally separable cadherin-catenin and Eph signaling modules (Figure 7). In contrast, in mammalian cortex a single class of extrinsic cues, sempahorins, coordinately controls the dendritic and axonal patterning of pyramidal neurons (Polleux et al., 2000). The existence of distinct somato-dendritic and axonal patterning modules could therefore be a specialized feature of motor circuit assembly, prompted by the dual compartmental environment of motor neurons.

Experimental Procedures

Mouse strains

γ-catenin conditional mutant (*γ-cat^flox*) mice were generated by gene targeting (Figure S1). Other mouse lines used: *β-cat^flox* (Brault et al., 2001), *γ-cat^−/−* (Ruiz et al., 1996), *Olig2::Cre* (Dessaud et al, 2007), *Hb9::eGFP* (Wichterle et al., 2002), *BAT-gal* (Maretto et al., 2003), *Catnb^lox(ex3)* (Harada et al., 1999) and *N-cad^flox* (Kostetskii et al., 2005).

In situ hybridization histochemistry and immunohistochemistry

In situ hybridizaton histochemistry was performed on 12μm cryostat sections using digoxigenin (DIG) labeled cRNA probes (Dasen et al., 2008). DNA templates for mouse *E-cad*, *T-cad, cad-8, cad-10, cad-20* and c*ad-22* were provided by S. Price. Templates for *β-cat, cad-6* and *cad-11* were cloned from cDNAs. Templates for mouse *N-cad, R-cad, VE-cad*, *cad-7, cad-9, cad-12, cad-15, cad-17, cad-18, cad-19*, and *γ-cat* were generated by RT-

PCR, and cloned into pCR-TOPO vectors (Invitrogen). Anti-sense DIG-cRNA probes were generated from DNA templates, using a DIG RNA Labeling Kit (Roche).

Immunohistochemistry was performed on 12μm cryostat sections using fluorophore-conjugated secondary antibodies (Jackson Labs and Invitrogen). Images were acquired on a Zeiss LSM510 confocal microscope. Antibodies described in Supplemental Experimental Procedures.

Analysis of motor neuron clustering and mixing

Neuronal mixing indices for segregation of LMC neurons are described in Supplemental Experimental Procedures.

Retrograde labeling of motor neurons

Embryos (e11.5 to e14.5) were injected with a 10% rhodamine-dextran (3K MW) solution into individual hindlimb muscles and incubated for 3–5h at 27°C before processing.

Motor neurite outgrowth

Motor neurons were derived from e10.5 embryos carrying an *Hb9::GFP* allele, and plated on a confluent monolayer of naïve or *N-cad* transfected CHO cells, and cultured for 16–20h in medium supplemented with trophic factors. GFP$^+$ neurite length was determined using MetaMorph software (Molecular Devices).

Supplementary Material

Refer to Web version on PubMed Central for supplementary material.

Acknowledgments

References

Brault V, Moore R, Kutsch S, Ishibashi M, Rowitch DH, McMahon AP, Sommer L, Boussadia O, Kemler R. Inactivation of the beta-catenin gene by Wnt1-Cre-mediated deletion results in dramatic brain malformation and failure of craniofacial development. Development. 2001; 128:1253–1264. [PubMed: 11262227]

Butz S, Stappert J, Weissig H, Kemler R. Plakoglobin and beta-catenin: distinct but closely related. Science. 1992; 257:1142–1144. [PubMed: 1509266]

Dasen JS, De Camilli A, Wang B, Tucker PW, Jessell TM. Hox repertoires for motor neuron diversity and connectivity gated by a single accessory factor, FoxP1. Cell. 2008; 134:304–316. [PubMed: 18662545]

De Marco Garcia NV, Jessell TM. Early motor neuron pool identity and muscle nerve trajectory defined by postmitotic restrictions in Nkx6.1 activity. Neuron. 2008; 57:217–231. [PubMed: 18215620]

Dessaud E, Yang LL, Hill K, Cox B, Ulloa F, Ribeiro A, Mynett A, Novitch BG, Briscoe J. Interpretation of the sonic hedgehog morphogen gradient by a temporal adaptation mechanism. Nature. 2007; 450:717–720. [PubMed: 18046410]

Grigoryan T, Wend P, Klaus A, Birchmeier W. Deciphering the function of canonical Wnt signals in development and disease: conditional loss- and gain-of-function mutations of beta-catenin in mice. Genes Dev. 2008; 22:2308–2341. [PubMed: 18765787]

Haegel H, Larue L, Ohsugi M, Fedorov L, Herrenknecht K, Kemler R. Lack of beta-catenin affects mouse development at gastrulation. Development. 1995; 121:3529–3537. [PubMed: 8582267]

Harada N, Tamai Y, Ishikawa T, Sauer B, Takaku K, Oshima M, Taketo MM. Intestinal polyposis in mice with a dominant stable mutation of the beta-catenin gene. EMBO J. 1999; 18:5931–5942. [PubMed: 10545105]

Huber AH, Weis WI. The structure of the beta-catenin/E-cadherin complex and the molecular basis of diverse ligand recognition by beta-catenin. Cell. 2001; 105:391–402. [PubMed: 11348595]

Imai T, Sakano H, Vosshall LB. Topographic mapping--the olfactory system. Cold Spring Harb Perspect Biol. 2010; 2:a001776. [PubMed: 20554703]

Jossin Y, Cooper JA. Reelin, Rap1 and N-cadherin orient the migration of multipolar neurons in the developing neocortex. Nat Neurosci. 2011; 14:697–703. [PubMed: 21516100]

Kadowaki M, Nakamura S, Machon O, Krauss S, Radice GL, Takeichi M. N-cadherin mediates cortical organization in the mouse brain. Dev Biol. 2007; 304:22–33. [PubMed: 17222817]

Kania A, Jessell TM. Topographic motor projections in the limb imposed by LIM homeodomain protein regulation of ephrin-A:EphA interactions. Neuron. 2003; 38:581–596. [PubMed: 12765610]

Kemler R. From cadherins to catenins: cytoplasmic protein interactions and regulation of cell adhesion. Trends Genet. 1993; 9:317–321. [PubMed: 8236461]

Kostetskii I, Li J, Xiong Y, Zhou R, Ferrari VA, Patel VV, Molkentin JD, Radice GL. Induced deletion of the N-cadherin gene in the heart leads to dissolution of the intercalated disc structure. Circ Res. 2005; 96:346–354. [PubMed: 15662031]

Ladle DR, Pecho-Vrieseling E, Arber S. Assembly of motor circuits in the spinal cord: driven to function by genetic and experience-dependent mechanisms. Neuron. 2007; 56:270–283. [PubMed: 17964245]

Lance-Jones C, Landmesser L. Motoneurone projection patterns in the chick hind limb following early partial reversals of the spinal cord. J Physiol. 1980; 302:581–602. [PubMed: 7411470]

Landmesser L. The distribution of motoneurones supplying chick hind limb muscles. J Physiol. 1978; 284:371–389. [PubMed: 731549]

Luo L, Flanagan JG. Development of continuous and discrete neural maps. Neuron. 2007; 56:284–300. [PubMed: 17964246]

Luria V, Krawchuk D, Jessell TM, Laufer E, Kania A. Specification of motor axon trajectory by ephrin-B:EphB signaling: symmetrical control of axonal patterning in the developing limb. Neuron. 2008; 60:1039–1053. [PubMed: 19109910]

Machon O, van den Bout CJ, Backman M, Kemler R, Krauss S. Role of beta-catenin in the developing cortical and hippocampal neuroepithelium. Neuroscience. 2003; 122:129–143. [PubMed: 14596855]

Maretto S, Cordenonsi M, Dupont S, Braghetta P, Broccoli V, Hassan AB, Volpin D, Bressan GM, Piccolo S. Mapping Wnt/beta-catenin signaling during mouse development and in colorectal tumors. Proc Natl Acad Sci U S A. 2003; 100:3299–3304. [PubMed: 12626757]

Megason SG, McMahon AP. A mitogen gradient of dorsal midline Wnts organizes growth in the CNS. Development. 2002; 129:2087–2098. [PubMed: 11959819]

Nelson WJ. Regulation of cell-cell adhesion by the cadherin-catenin complex. Biochem Soc Trans. 2008; 36:149–155. [PubMed: 18363555]

Nelson WJ, Nusse R. Convergence of Wnt, beta-catenin, and cadherin pathways. Science. 2004; 303:1483–1487. [PubMed: 15001769]

Palmesino E, Rousso DL, Kao TJ, Klar A, Laufer E, Uemura O, Okamoto H, Novitch BG, Kania A. Foxp1 and lhx1 coordinate motor neuron migration with axon trajectory choice by gating Reelin signalling. PLoS Biol. 2010; 8:e1000446. [PubMed: 20711475]

Patel SD, Ciatto C, Chen CP, Bahna F, Rajebhosale M, Arkus N, Schieren I, Jessell TM, Honig B, Price SR, et al. Type II cadherin ectodomain structures: implications for classical cadherin specificity. Cell. 2006; 124:1255–1268. [PubMed: 16564015]

Personius KE, Chang Q, Mentis GZ, O'Donovan MJ, Balice-Gordon RJ. Reduced gap junctional coupling leads to uncorrelated motor neuron firing and precocious neuromuscular synapse elimination. Proc Natl Acad Sci U S A. 2007; 104:11808–11813. [PubMed: 17609378]

Pitkanen A, Savander V, LeDoux JE. Organization of intra-amygdaloid circuitries in the rat: an emerging framework for understanding functions of the amygdala. Trends Neurosci. 1997; 20:517–523. [PubMed: 9364666]

Polleux F, Morrow T, Ghosh A. Semaphorin 3A is a chemoattractant for cortical apical dendrites. Nature. 2000; 404:567–573. [PubMed: 10766232]

Price SR, Briscoe J. The generation and diversification of spinal motor neurons: signals and responses. Mech Dev. 2004; 121:1103–1115. [PubMed: 15296975]

Price SR, De Marco Garcia NV, Ranscht B, Jessell TM. Regulation of motor neuron pool sorting by differential expression of type II cadherins. Cell. 2002; 109:205–216. [PubMed: 12007407]

Romanes GJ. The motor pools of the spinal cord. Prog Brain Res. 1964; 11:93–119. [PubMed: 14300484]

Ruiz P, Brinkmann V, Ledermann B, Behrend M, Grund C, Thalhammer C, Vogel F, Birchmeier C, Gunthert U, Franke WW, et al. Targeted mutation of plakoglobin in mice reveals essential functions of desmosomes in the embryonic heart. J Cell Biol. 1996; 135:215–225. [PubMed: 8858175]

Sperry RW. Chemoaffinity in the orderly growth of nerve fiber patterns and connections. Proc Natl Acad Sci U S A. 1963; 50:703–710. [PubMed: 14077501]

Surmeli G, Akay T, Ippolito AG, Tucker PW, Jessell TM. Patterns of sensory-motor connectivity prescribed by a dorsoventral positional template. Cell. 2011 Submitted.

Takai Y, Nakanishi H. Nectin and afadin: novel organizers of intercellular junctions. J Cell Sci. 2003; 116:17–27. [PubMed: 12456712]

Vanderhorst VG, Holstege G. Organization of lumbosacral motoneuronal cell groups innervating hindlimb, pelvic floor, and axial muscles in the cat. J Comp Neurol. 1997; 382:46–76. [PubMed: 9136811]

Wichterle H, Lieberam I, Porter JA, Jessell TM. Directed differentiation of embryonic stem cells into motor neurons. Cell. 2002; 110:385–397. [PubMed: 12176325]

Yip YP, Mehta N, Magdaleno S, Curran T, Yip JW. Ectopic expression of reelin alters migration of sympathetic preganglionic neurons in the spinal cord. J Comp Neurol. 2009; 515:260–268. [PubMed: 19412957]

Zelano J, Wallquist W, Hailer NP, Cullheim S. Expression of nectin-1, nectin-3, N-cadherin, and NCAM in spinal motoneurons after sciatic nerve transection. Exp Neurol. 2006; 201:461–469. [PubMed: 16777094]

Zhurinsky J, Shtutman M, Ben-Ze'ev A. Plakoglobin and beta-catenin: protein interactions, regulation and biological roles. J Cell Sci. 2000; 113:3127–3139. [PubMed: 10954412]
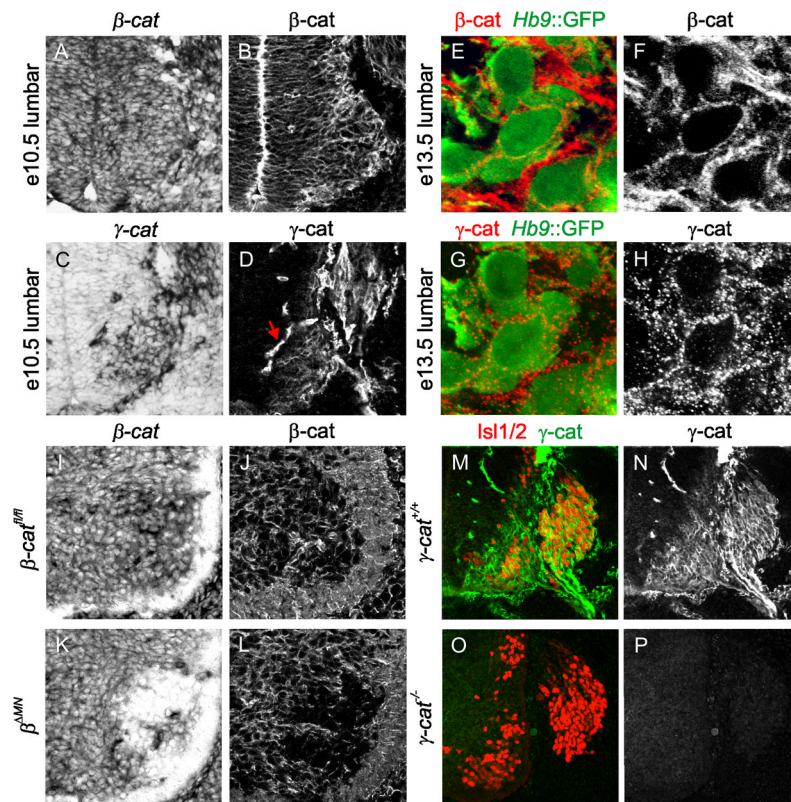
Figure 1. β- and γ-catenin expression in developing motor neurons

A,B. β-catenin (β-cat) expression in e10.5 lumbar spinal cord.

C,D. γ-catenin (γ-cat) expression in e10.5 lumbar spinal cord. Arrow marks blood vessels. Between e15.5 and p0, *γ-catenin* transcript is extinguished from most spinal motor neurons (Figure S1E–H).

E–H. β-cat and γ-cat expression in GFP+ lumbar motor neurons in e13.5 *Hb9::GFP* transgenic mice.

I,K. *β-cat* expression in e13.5 lumbar spinal cord from control *β-cat^{fl/fl}* and *β^{ΔMN}* embryos.

J,L. β-cat expression in e13.5 lumbar spinal cord from control *β-cat^{fl/fl}* and *β^{ΔMN}* embryos. In the absence of motor neuron β-catenin expression we observed a marked upregulation of γ-catenin protein (Figure S1I–L).

M–P. Absence of γ-cat expression in e11.5 lumbar spinal cord of *γ-cat^{−/−}* mice.

RNA expression data in panels A, C, I and K with positive signal in black.
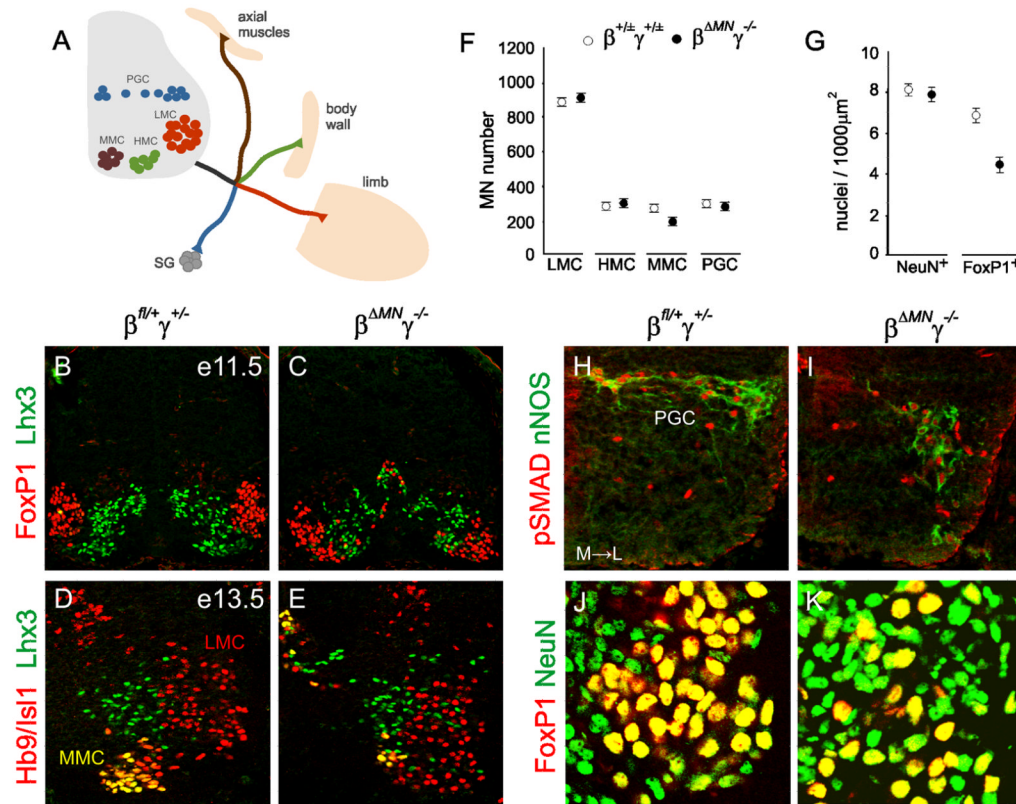
Figure 2. Motor neuron columnar segregation in β- and γ-catenin mutants

A. Topographic order in motor innervation of the mouse limb: median motor column (MMC) neurons innervate axial muscles, hypaxial motor column (HMC) neurons innervate body wall muscles, lateral motor column (LMC) neurons innervate limb muscles, and preganglionic motor column (PGC) neurons innervate sympathetic ganglion (SG) neurons.

B–C. Segregation of Lhx3$^+$ MMC and FoxP1$^+$ LMC neurons at lumbar levels of e11.5 control and $\beta^{\Delta MN}\gamma^{-/-}$ embryos.

D–E. Segregation of Lhx3$^+$, Hb9$^+$, Isl1$^+$ MMC and Hb9$^+$, Isl1$^+$ LMC neurons at lumbar levels of e13.5 control and $\beta^{\Delta MN}\gamma^{-/-}$ embryos.

F. Post-mitotic motor neurons in the marginal zone of e13.5 spinal cord of control ($\beta^{+/\pm}\gamma^{+/\pm}$) and $\beta^{\Delta MN}\gamma^{-/-}$ embryos. Motor neurons/100μm: mean +/− SEM (difference from control significant for MMC neurons; t-test, p<0.0001). Control catenin group ($\beta^{+/\pm}\gamma^{+/\pm}$) includes genotypes: $\beta^{+/+}\gamma^{+/+}$ (wt), $\beta^{+/\Delta MN}\gamma^{+/+}$, $\beta^{+/+}\gamma^{+/-}$ and $\beta^{+/\Delta MN}\gamma^{+/-}$.

G. NeuN$^+$ and FoxP1$^+$ neuronal densities in the LMC of e13.5 control and $\beta^{\Delta MN}\gamma^{-/-}$ embryos; mean +/− SEM (t-test, p<0.001 vs control for FoxP1$^+$ density).

H–I. pSMAD$^+$, nNOS$^+$ PGC neurons in e13.5 control and $\beta^{\Delta MN}\gamma^{-/-}$ embryos.

J–K. NeuN$^+$, FoxP1^{off} and NeuN$^+$, FoxP1$^+$ neurons within the LMC in e13.5 of control and $\beta^{\Delta MN}\gamma^{-/-}$ embryos.
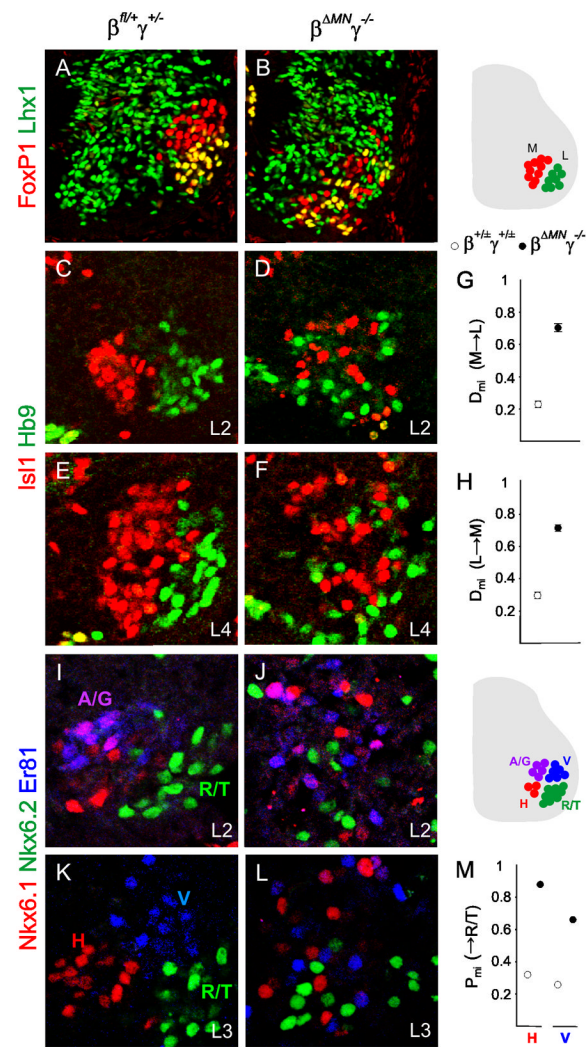
**Figure 3. Impaired LMC divisional and pool segregation in β- and γ-catenin mutants**

A,B. FoxP1$^+$, Lhx1^{off} medial, and FoxP1$^+$, Lhx1$^+$ lateral LMC neurons in e11.5 control and $\beta^{\Delta MN}\gamma^{-/-}$ embryos.

C–F. Isl1$^+$ medial and Hb9$^+$ lateral LMC neurons at lumbar (L)2 and L4 levels in e13.5 control and $\beta^{\Delta MN}\gamma^{-/-}$ embryos.

G,H. Divisional mixing indices (D$_{mi}$) of medial→lateral and lateral→medial LMC neurons in e13.5 control (○) and $\beta^{\Delta MN}\gamma^{-/-}$ (●) embryos; mean +/− SEM (t-test, p<0.0001 for M→L and L→M).

I–L. LMC pools at L2 and L4 levels in e13.5 control and $\beta^{\Delta MN}\gamma^{-/-}$ embryos. Nkx6.1$^+$, Er81$^+$adductor/gracilis (A/G) neurons; Er81$^+$, Nkx6.1^{off} vasti (V) neurons; Nkx6.2$^+$ rectus femoris/tensor fasciae latae (R/T) neurons; and Nkx6.1$^+$, Er81^{off} hamstring (H) motor neurons.

M. Pool mixing indices (P$_{mi}$) of H→R/T and V→R/T pools in e13.5 control (○) and $\beta^{\Delta MN}\gamma^{-/-}$ (●) embryos (χ^2 test, p<0.0001 for H→R/T and V→R/T). See also Table S4.
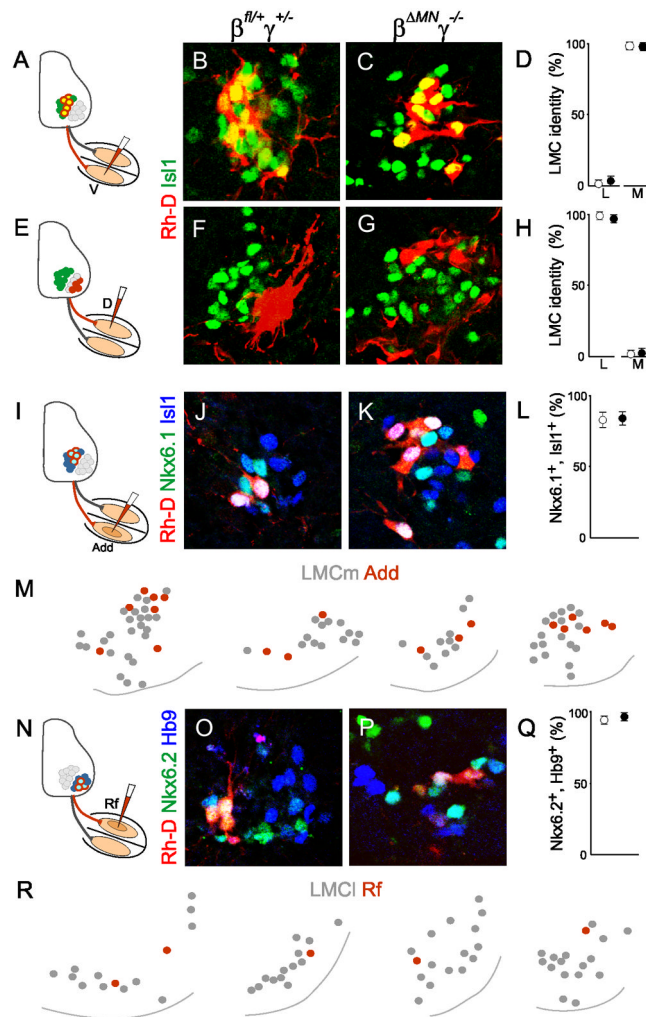
Figure 4. Link between motor neuron transcriptional identity and axonal trajectory is preserved in β- and γ-catenin mutants

A–D. Medial LMC (Isl1$^+$) status of Rh-D labeled motor neurons after tracer injection into ventral limb of e13.5 control and $\beta^{\Delta MN}\gamma^{-/-}$ embryos.

E–H. Lateral LMC (Isl1^{off}) status of Rh-D labeled motor neurons after tracer injection into dorsal limb of e13.5 control and $\beta^{\Delta MN}\gamma^{-/-}$ embryos.

I–L. Nkx6.1$^+$, Isl1$^+$ status of Rh-D labeled LMC neurons after tracer injection into adductor magnus (Add) muscle at e13.5 in control and $\beta^{\Delta MN}\gamma^{-/-}$ embryos.

M. Position of Rh-D labeled Add motor neurons within the medial LMC in $\beta^{\Delta MN}\gamma^{-/-}$ embryos.

N–Q. Nkx6.2$^+$, Hb9$^+$ status of Rh-D labeled LMC neurons after tracer injection into rectus femoris (Rf) muscle at e13.5 in control and $\beta^{\Delta MN}\gamma^{-/-}$ embryos.

R. Position of Rh-D labeled Rf motor neurons within the lateral LMC in $\beta^{\Delta MN}\gamma^{-/-}$ embryos. Values in D, H, L and Q show mean +/− SEM.
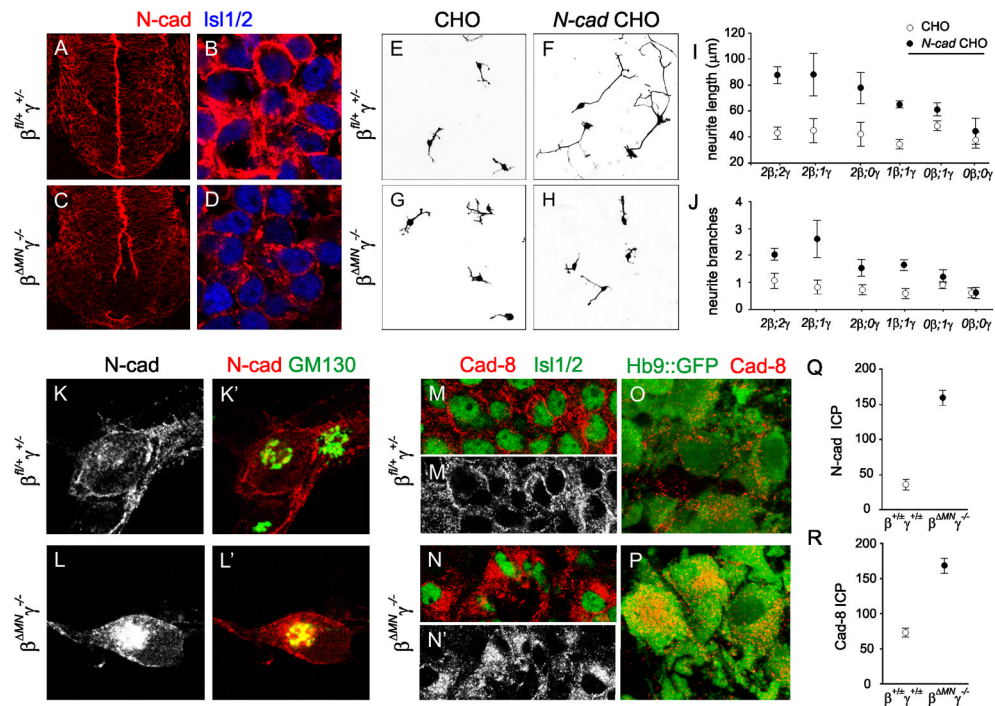
Figure 5. β- and γ-catenin inactivation perturbs cadherin localization and function

A–D. N-cad localization of Isl1/2$^+$ lumbar motor neurons in e10.5 control and $\beta^{\varDelta MN}\gamma^{-/-}$ embryos.

E–H. Neurite outgrowth of motor neurons dissociated from e10.5 *Hb9::GFP* embryos and seeded on monolayers of naïve or N-cad-expressing CHO cells. Motor neurons visualized by GFP immunoreactivity depicted in black.

I, J. Neurite length and branching for control and compound catenin mutants (genotypes indicate the number of wild-type alleles) grown on naive (○) or N-cad (●) expressing CHO cells; mean +/− SEM (t-test, p>0.05 for all genotypes except $\beta^{\varDelta MN}\gamma^{+/-}$ and $\beta^{\varDelta MN}\gamma^{-/-}$).

K–L′. N-cad co-localization with the Golgi marker GM130 in motor neurons dissociated from e10.5 control and $\beta^{\varDelta MN}\gamma^{-/-}$ embryos.

M–N′. Cad-8 localization in Isl1/2$^+$ motor neurons of e13.5 control and $\beta^{\varDelta MN}\gamma^{-/-}$ embryos.

O,P. Cad-8 co-localization with GFP in motor neurons of control and $\beta^{\varDelta MN}\gamma^{-/-}$ embryos expressing a *Hb9::eGFP* transgene.

Q,R. Intracellular N-cad and cad-8 levels in e13.5 motor neurons from control and $\beta^{\varDelta MN}\gamma^{-/-}$ embryos. Values indicate intracellular pixel (ICP) intensity, +/− SEM (t-test, p<0.0001).
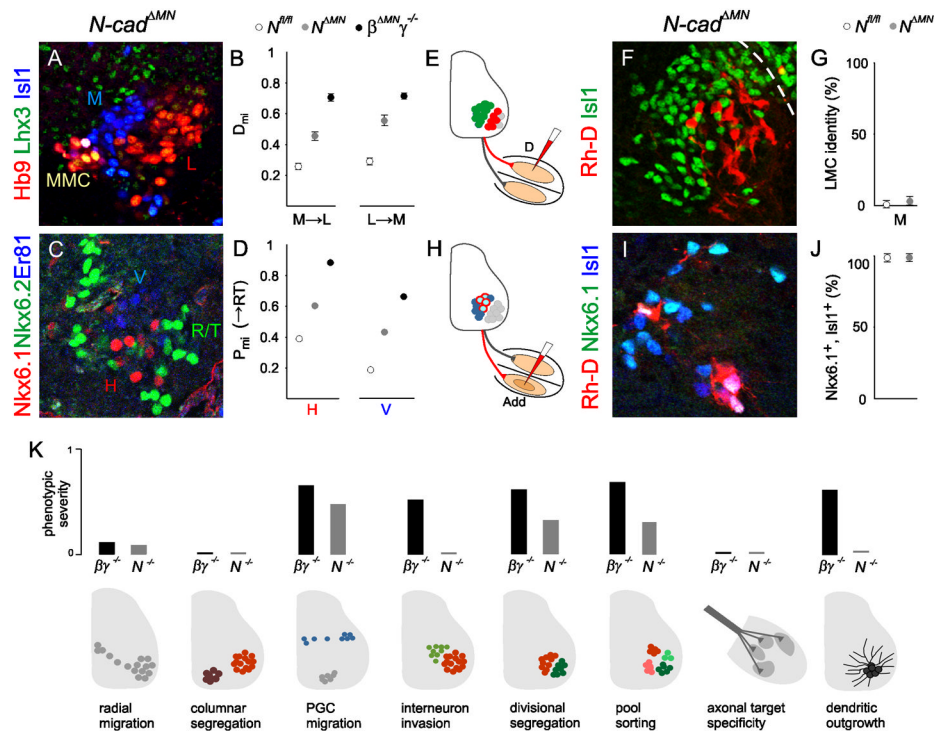
Figure 6. Disorganization of LMC neuronal position in N-cadherin mutants

A. Organization of Isl1$^+$, Hb9^{off}, Lhx3^{off} medial and Hb9$^+$, Isl1^{off}, Lhx3^{off} lateral LMC neurons in e13.5 *N-cad^{ΔMN}* embryos.

B. Divisional mixing indices of medial→lateral and lateral→medial LMC neurons in control, *N-cad^{ΔMN}*, and *β^{ΔMN}γ$^{-/-}$*embryos; mean +/− SEM (t-test, p<0.0001 for control vs *N-cad^{ΔMN}*, and p<0.0001 for *N-cad^{ΔMN}* vs *β^{ΔMN}γ$^{-/-}$*).

C. Motor pool organization in e13.5 *N-cad^{ΔMN}* embryos (pool markers described in Figure 3I–L).

D. Pool mixing indices (P$_{mi}$) from R/T→H, and R/T→V pool comparisons in e13.5 control, *N-cad^{ΔMN}*, and *β^{ΔMN}γ$^{-/-}$*embryos, (χ^2 test, p<0.0001 for all comparison between controls and *N-cad^{ΔMN}* and for R/T→V between *N-cad^{ΔMN}* and *β^{ΔMN}γ$^{-/-}$*, p<0.01 for R/T→H between *N-cad^{ΔMN}* and *β^{ΔMN}γ$^{-/-}$*).

E–G. Isl1$^+$ medial LMC status of Rh-D labeled motor neurons after tracer injection into dorsal limb mesenchyme of e13.5 *N-cad^{ΔMN}* embryos. Dotted line in F indicates spinal cord/DRG separation. Values in G show mean +/− SEM.

H–J. Nkx6.1$^+$, Isl1$^+$ status of Rh-D labeled LMC neurons after tracer injection into adductor magnus muscle of e13.5 *N-cad^{ΔMN}* embryos. Values in J show mean +/− SEM.

K. Phenotypic severity in *β^{ΔMN}γ$^{-/-}$* and *N-cad^{ΔMN}* embryos indicated by the height of bars (y-axis scale is not quantitative).
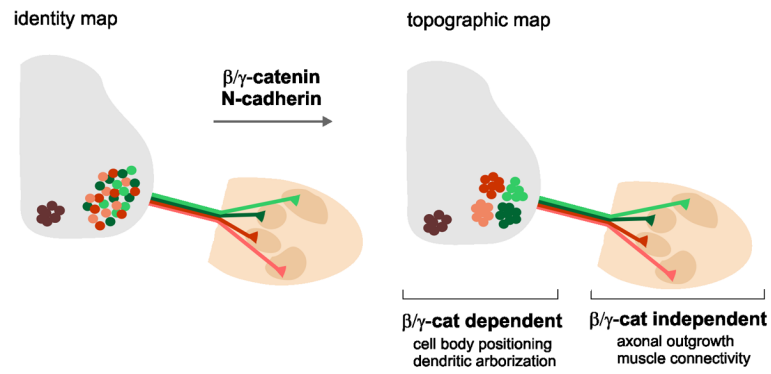
Figure 7. β- and γ-catenin activities promote topographic motor mapping

Catenin-dependent positioning of motor pools promotes topographic motor mapping. In the absence of catenin function, neuromuscular mapping reverts to an identity-based plan. Moreover, catenins appear to control central but not peripheral programs of motor neuron patterning. Key: MMC, brown; LMCm, red; LMCl, green.